THE JOURNAL OF PHYSICAL CHEMISTRY A

Article

pubs.acs.org/JPCA

tert-Butyl Carbocation in Condensed Phases: Stabilization via Hyperconjugation, Polarization, and Hydrogen Bonding

Evgenii S. Stoyanov*[,†,‡] and Gabriel dos Passos Gomes[§]

[†]N. N. Vorozhtsov Novosibirsk Institute of Organic Chemistry, Siberian Branch of the Russian Academy of the Sciences (SB RAS), Novosibirsk 630090, Russia

[‡]Department of Natural Science, National Research University - Novosibirsk State University, Novosibirsk 630090, Russia

[§]Department of Chemistry and Biochemistry, Florida State University, Tallahassee, Florida 32306, United States

Supporting Information

ABSTRACT: Despite the seeming similarity of the infrared (IR) spectra between *tert*-butyl cations (*t*-Bu$^+$) in gaseous and condensed phases, there are important but so far unrecognized differences. The IR spectroscopic investigation of the hydrogen (H)-bonding of *t*-Bu$^+$ with the immediate environment together with the X-ray crystallographic data shows that one CH_3 group of *t*-Bu$^+$ differs from the other two. In the Ar-tagged *t*-Bu$^+$ in vacuum, this group is predominantly polarized, showing three C−H stretch vibrations at 2913, 2965, and 3036 cm^{-1} whereas the other two methyls are predominantly involved in strong hyperconjugation, yielding an intense triple IR band with a maximum at 2839 cm^{-1}. In a condensed phase, the bulk solvent effect promoted participation of the polarized CH_3 group in additional hyperconjugation, decreasing its νCH_3 frequencies by approximately 120 cm^{-1}, whereas frequencies of the other CH_3 groups decreased by only ca. 4−10 cm^{-1}. This observation indicates that the influence of the condensed phase on *t*-Bu$^+$ stabilization is substantial. Thus, enhancement of H-bonding between *t*-Bu$^+$ and Anion$^-$ strengthens hyperconjugation and promotes further cation stabilization.

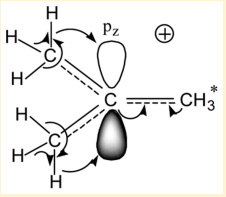

1. INTRODUCTION

Carbocations are widely known to be reaction intermediates in acid-catalyzed hydrocarbon reactions that are of prime importance to the petrochemical industry.[1] The first experimental exploration of carbocations in liquid superacids by nuclear magnetic resonance (NMR) and infrared (IR) spectroscopy was performed by Olah et al. in the 1960s.[2,3] Since that time, the carbocations and their stability have been extensively studied theoretically[4−11] and in the gas phase by mass spectrometry.[12−14] The most stable cation, *tert*-butyl (*t*-Bu$^+$), received the most attention. The existence of an intense low-frequency band of CH stretches at 2830 cm^{-1} (hereafter referred to as νCH_{max}) in the IR spectrum of *t*-Bu$^+$ in superacid SbF_5 matrices has been assumed to be evidence of hyperconjugation.[2] The close resemblance of the empirical gaseous-phase IR spectrum of the *t*-Bu$^+$ cation (with νCH_{max} at 2834 cm^{-1}) tagged with argon[8] with that calculated under conditions of C_s symmetry[7,9,10] suggests that the specific features of the IR spectrum of the gaseous *t*-Bu$^+$ cation and the mechanism of its stabilization have been finally identified: The positive charge is delocalized via hyperconjugated interaction of the three C−H bonds—one from each of the three CH_3 groups—with the empty p_z orbital of the central sp^2 carbon atom.[6−10] These three C−H bonds are aligned in parallel with the p_z orbital and donate its σ-electron density resulting in strong σ−p_z hyperconjugation (Scheme 1). Their frequencies are observed as an intense characteristic νCH_{max} band. The other six C−H bonds (formally designated as "free") should develop the high frequency bands $\nu_{as}CH_2$ (3036 cm^{-1}) and ν_sCH_2 (2965 cm^{-1}).[8]

Scheme 1. Illustration of Hyperconjugative Delocalization of the Positive Charge in the *tert*-Butyl Cation

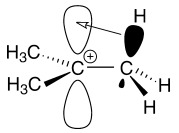

Such interpretation of the gaseous *t*-Bu$^+$ spectrum raises some issues requiring an explanation. For example, the σ−p_z hyperconjugation decreases the σ-electron density in the aligned C−H bonds, and decreases the νCH_{max} by *ca.* −120 cm^{-1} relative to the arbitrary $(CH_3)_4C$ molecule. At the same time, stretch vibrations of the other two "free" C−H bonds show a blue $\Delta\nu$CH shift of ca. +60 cm^{-1} with respect to that of$(CH_3)_4C$; i.e., the *e*-density of these bonds increases. Can this happen if all three C−H bonds have one shared C atom and form hybridized molecular orbitals? Calculations show that the blue shift may be caused by the rehybridization effect,[15,16] but manifestation of the blue shift is expected to be much weaker. Another issue is the questionable conclusion that is based on close similarity of νCH_{max} in the spectra of *t*-Bu$^+$ in the gas phase (2834 cm^{-1}),[8] in a liquid superacidic SbF_5 matrix (2830 cm^{-1}),[2] and in the *t*-Bu$^+$[Sb_2F_{11}]$^-$ salt (2830 cm^{-1}):[17] the bulk solvent effect and the crystal lattice do not affect *t*-Bu$^+$. Meanwhile, in solid-phase IR spectra, the bands corresponding

Received: May 15, 2015
Revised: July 9, 2015

ACS Publications © XXXX American Chemical Society

DOI: 10.1021/acs.jpca.5b04657
J. Phys. Chem. A XXXX, XXX, XXX−XXX

to vibrations of "free" C−H bonds almost disappear.[18] Moreover, recently it was shown that the *t*-Bu$^+$ cation forms sufficiently strong H-bonds with counterions in its solid salts,[18] thus confirming that the influence of the environment on the *t*-Bu$^+$ is significant and may be an additional factor affecting its stabilization. Therefore, the seeming similarity of IR spectra of *t*-Bu$^+$ in vacuum and in condensed phases requires an explanation. The available X-ray structures of *t*-Bu$^+$ cannot provide exhaustive answers because the hydrogen positions have not been refined.[19−22] Similarly, the quick hydrogen exchange in H^1 NMR also limits the usefulness of this method. The method of IR spectroscopy is informative because C−H stretch and bend vibrations of the *t*-Bu$^+$ cation are sensitive to all effects of its stabilization.

In the present work, we identified correlations between the features of IR spectra of the *t*-Bu$^+$ cation and its X-ray crystallographic structure and explored dependencies of C−H vibrations on the basicity of the solvated surroundings in a solid phase and in solutions. Comparison of empirical IR spectra with those calculated for optimized C_s and C_1 conformers of neat *t*-Bu$^+$ and of *t*-Bu$^+$ solvated with Ar (natural bond orbital analysis, B3LYP/6-31G++[d,p] calculations) allowed us to clearly demonstrate their inconsistency and to gain deeper insights into the mechanism of *t*-Bu$^+$ stabilization. Other levels of calculations[7,8] can refine the optimized structures of *t*-Bu$^+$, without affecting the major discrepancies between the calculated and empirical IR spectra.

We chose the salts of the *t*-Bu$^+$ cation with carborane counterions because of their exceptionally high stability at low basicity.[23] The structures of carborane (abbreviated as Carb$^-$) with the total formula $CHB_{11}X_{11}^-$ (where X = F, Cl, or Br) and $CHB_{11}R_5X_6^-$ (where R = H or CH_3 and X = Cl or Br) are shown in Scheme 2. Because all Carb$^-$ anions contain the CHB_{11} cage, we omitted it in formulas, instead using abbreviated symbols $\{X_{11}^-\}$ and $\{R_5X_6^-\}$.

Scheme 2. Icosahedral Carborane Anions of the Type $CHB_{11}X_{11}^-$ (a) and $CHB_{11}R_5X_6^-$ (b) That We Used in This Work (Abbreviated as $\{X_{11}^-\}$ and $\{R_5X_6^-\}$, Respectively)

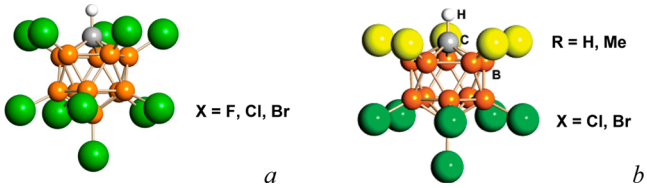

2. EXPERIMENTAL SECTION

The carborane acids as precursors for synthesis of *t*-Bu$^+$ salts were prepared as described previously.[24,25] The *t*-Bu$^+\{F_{11}^-\}$ and *t*-Bu$^+\{Cl_{11}^-\}$ salts were prepared as follows:[18,25] gaseous C_2H_5Cl was allowed to react with the sublimed acid and formed chloronium salts $(C_2H_5)_2Cl^+\{X_{11}^-\}$ (X = F, Cl), which were then decomposed at 100 °C in 10^{-5} Torr vacuum in accordance with eq 1:

$$(C_2H_5)_2Cl^+\{X_{11}^-\} \rightarrow C_4H_9^+\{X_{11}^-\} + HCl \quad (1)$$

This method yields highly pure $C_4H_9^+\{X_{11}^-\}$ salts. Larger-scale synthesis of these salts and that of the $C_4H_9^+\{Br_{11}^-\}$ salt were accomplished via a direct reaction of the corresponding carborane acids with 1Cl-butane, followed by washing of the white product with cold dichloromethane. The *t*-Bu$^+\{Cl_{11}^-\}$ crystals were grown in 1,1,2,2-tetrachloroethane solutions.

All procedures were performed in a Vacuum Atmospheres Corp. glovebox in the atmosphere of He (O_2 and H_2O < 0.5 ppm). IR spectra were recorded on a PerkinElmer Spectrum-100 spectrometer inside a drybox in either transmission or attenuated total reflectance (ATR) mode (450−4000 cm^{-1}). The spectra of saturated solutions of *t*-Bu$^+\{F_{11}^-\}$ and *t*-Bu$^+\{Cl_{11}^-\}$ in dichloroethane-d_4 were recorded in the cell with Si windows, with subtraction of the solvent spectrum. The IR spectra of *t*-Bu$^+\{R_5X_6^-\}$ salts ($\{R_5X_6^-\}$ = $\{Me_5Cl_6^-\}$, $\{Me_5Br_6^-\}$, or $\{H_5Br_6^-\}$) were obtained from the samples that we studied earlier.[20] The IR data were processed in the GRAMMS/A1 (7.00) software from Thermo Scientific. ^1H NMR spectra were recorded on a Varian Inova 500.

All computations were performed in the Gaussian 03 software[26] with the hybrid functional B3LYP and the 6-31G++(d,p) basis set. Chemcraft 1.7[27] and CYLView[28] were used to render the molecules. The NBO 3.0 software[29] was used to analyze electron properties and orbital interactions of *t*-Bu$^+$.

3. RESULTS AND DISCUSSION

3.1. Characterization of *t*-Bu$^+$ on the Basis of Calculations. *Neat t-Bu*$^+$. The optimized conformers of *t*-Bu$^+$ at the B3LYP/6-311G++(d,p) level and in NBO analysis, in accordance with other studies,[7,8] correspond to the C_s (lower energy) and C_1 (slightly higher energy) symmetry. In the more symmetric C_s structure, one of C−H bonds in each methyl group is coplanar to the empty p_z-orbital and thus is the best hyperconjugative donor yielding the greatest stabilization of the cationic center (from ∼23 to ∼21 kcal for different methyl groups; Figure S1, Supporting Information). The other two C−H bonds in each methyl group are positioned symmetrically relative to the empty p_z-orbital at a dihedral angle. This situation allows both of them to engage in much weaker hyperconjugation with the cationic center (2.2 × 2 and [1.9 + 3.1] × 2 kcal/mol). Hyperconjugation weakened the C−H bond and elongated it.

Figure 1 shows a correlation diagram between the calculated spectra of tetramethylmethane and of the C_s isomer of *t*-Bu$^+$. One can see that decreasing the local symmetry of the CH_3 group from C_{3v} for $C(CH_3)_4$ to C_s for *t*-Bu$^+$ reduces the symmetric C−H stretch from 3028 to 2981 cm^{-1}, respectively

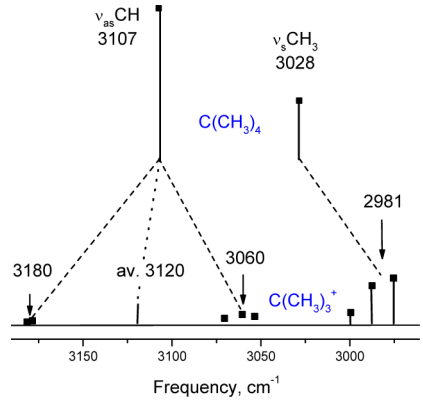

Figure 1. Correlation diagram between the calculated spectra at the B3LYP/6-311G++(d,p) level for stretch vibrations of CH_3 groups of tetramethylmethane (local symmetry C_{3v}) and those of the C_s isomer of *t*-Bu$^+$.

DOI: 10.1021/acs.jpca.5b04657
J. Phys. Chem. A XXXX, XXX, XXX−XXX

(by ~47 cm^{-1}), with splitting into three components. This phenomenon occurs because three C−H bonds that are best aligned with the p_z orbital are mostly weakened and their stretches mostly decrease. The vibrations of unaligned C−H bonds at 3180 and ca. 3060 cm^{-1}, which originate from $\nu_{as}CH_3$ of $C(CH_3)_4$ at 3107 cm^{-1}, are blue-shifted by 13 cm^{-1} on average, even though their involvement should facilitate a red shift of their stretches. This phenomenon can be explained by the rehybridization effect.

Rehybridization is a stereoelectronic effect, not recognized in the earlier studies on *t*-Bu^+, and this effect is closely associated with hyperconjugation (or a lack thereof). This effect manifests itself as a dramatic difference in hybridization of C−H bonds as a function of their orientation relative to the p_z-orbital. The range of hybridization values for the C−H bonds in the methyl groups is significant: from $sp^{3.96}$ (20.3% s-character) to $sp^{2.91}$ (25.7% s-character). Because hybridization is well-known to correlate with C−H stretching frequencies,[30] we will briefly analyze the origin and scope of this stereoelectronic effect.

The most dramatically increased amount of the p-character (approaching sp^4) was found for C−H bonds aligned with the p_z orbital (Figure S1 in Supporting Information). Not only does the enhanced p-character render this C−H bond a better donor,[15,30] but it also decreases the C−C−H valence angle to ~103°, leading to better alignment with the empty p orbital. The tendency for rehybridization should lead to a noticeable blue-shift in frequencies of the C−H bonds misaligned with the p_z orbital. This effect can compensate or exceed the effect of hyperconjugation. The rehybridization effect is responsible, for example, for the increased CH stretch frequencies of those C−H bonds that are directly attached to the alkene and alkyne carbons.

t-Bu⁺ in a Condensed Phase without H-Bonding. The transfer of *t*-Bu^+ from vacuum to a condensed phase should affect its *e*-density distribution and IR spectrum. The influence of the condensed phase on *t*-Bu^+ results from its solvation by the immediate environment and from the effects of bulk properties of the condensed phase. We found that electron perturbations imposed by the IEF-PCM continuum solvation model (chloroform)[31,32] are minor. The calculated IR spectra show that in the condensed phase, compared to a vacuum, the CH stretches are decreased by 11−15 cm^{-1}, as expected (Table S1 in Supporting Information). The *t*-Bu^+ IR spectrum that was calculated on the basis of the dielectric polarized continuum solvation model (D-PCM),[33] which takes into account the electrostatic and dispersion−repulsion terms, actually does not show the one-directional changes in the frequencies of CH stretches (Table S1 in the Supporting Information).

The solvation may have a stronger influence on *t*-Bu^+. We simulated the *t*-Bu^+ solvation by Ar atoms in a vacuum, because basicity of Ar is lower or comparable with that of SbF_5, $Sb_2F_{11}^{2-}$, and $\{F_{11}^-\}$ ions, which solvate *t*-Bu^+ in liquid "magic" superacids and solid *t*-$Bu^+\{F_{11}^-\}$ salts.

Solvation of t-Bu⁺ with Ar. Binding of one Ar atom to the central C atom of *t*-Bu^+ or to the H atom of its CH_3 group does not lead to substantial differences in their IR spectra (Figure S2 and Table S2 in the Supporting Information). The most strongly affected C−H bonds show a red shift of νCH_{max} by 36 cm^{-1}.

Optimized structure of the trisolvate, *t*-Bu^+·3Ar, shows that Ar atoms are bound to the most strongly charged H atoms of the C−H bonds that are involved in strong hyperconjugation (Figure 2). Three frequencies are most strongly red-shifted

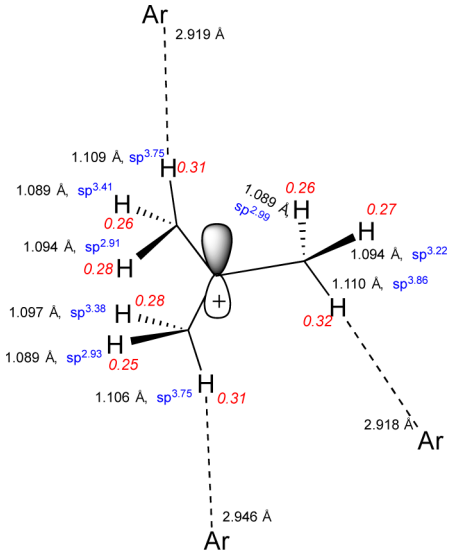

Figure 2. Optimized structure of *t*-Bu^+·3Ar at the B3LYP/6-311G++(d,p) level.

($\Delta\nu$) and yield the νCH_{max} band with $\Delta\nu$ ca. 39 cm^{-1}. The other frequencies, from unaligned C−H bonds, are less shifted: by ca. 28 and 7 cm^{-1} (Table S3 in the Supporting Information). Thus, the H-bonding of Ar atoms to aligned C−H bonds has a weak effect on CH stretches and on weakening of the rehybridization effect.

The calculated spectrum of the fully solvated cation, *t*-Bu^+·9Ar, compared to that for *t*-Bu^+·3Ar, shows a more uniform decrease in all frequencies of CH_3 groups; these reductions do not exceed 34 cm^{-1} (Table S2, Supporting Information). That is, additional solvation with six Ar atoms affects the cation weakly.

3.2. Empirical Structural and Spectral Features of *t*-Bu⁺. The IR spectrum of *t*-Bu^+ in gas[8] shows a high similarity with that in liquid[2,21] and solid[16] phases, mostly because of the presence of the intense νCH_{max} absorption. This phenomenon is illustrated in Figure 3, where deconvoluted spectra of the gaseous *t*-Bu^+ and of the solid *t*-$Bu^+\{F_{11}^-\}$ salt are compared. The gas-phase spectra should show more complex patterns because of the partially resolved rotational structure. In this case, the bands of CH stretches of *t*-Bu^+, shown in Figure 3a, should consist of a narrow central band and broader P and R branches. In the vibrational−rotational spectrum of isobutane, the distances from P and R branches to the central peek are 13 cm^{-1}; that is, the P−R distance is ca. 26 cm^{-1}. The same should be true for the *t*-Bu^+ cation. Nevertheless, the half-width of the νCH_{max} band is greater, 44 cm^{-1}, which means that the P and R branches are not resolved and merge into one band. The same should occur with all other bands.

Two bands, to the left and right of the central νCH_{max}, at 2881 and 2790 cm^{-1}, respectively (Figure 3a), cannot be the P and R branches because (a) they are separated by 90 cm^{-1}, i.e., much more than 26 cm^{-1}; (b) their intensity is 5-fold weaker than that of νCH_{max} (intensity levels of P and R are greater than that of the central peak); (c) their half-width, ca. 40 cm^{-1}, coincides with that of νCH_{max} (in case of P and R, the half-width would have to be much greater); and (d) their contours can be accurately interpreted as mixed Gaussian + Lorenzian (this is impossible for P and R contours). Thus, the IR spectrum resolution of gaseous *t*-Bu^+ is insufficient to

DOI: 10.1021/acs.jpca.5b04657
J. Phys. Chem. A XXXX, XXX, XXX−XXX

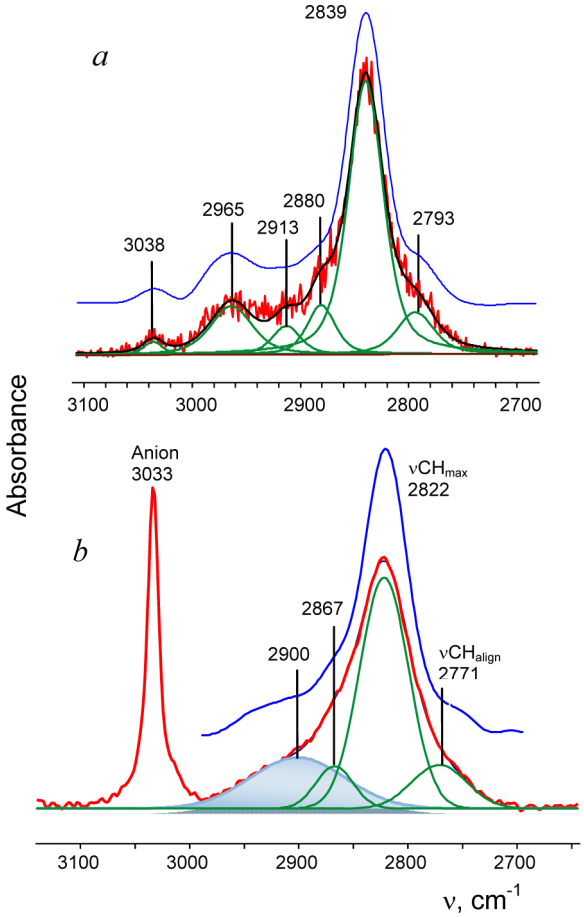

Figure 3. IR spectrum of the gaseous *t*-Bu$^+$ cation (a) (provided by the authors of ref 8 and published there) and that of the solid *t*-Bu$^+${F$_{11}^-$} salt (b). The spectra are separated into components with mixed Gaussian + Lorenzian (a) and Gaussian (b) contours. Blue denotes the spectra after application of the Deconvolve (FSD) procedure, which allows for narrowing of the components of the spectrum to uncover their existence more effectively. The broad absorption at ca. 2900 cm^{-1} is shown as shaded blue.

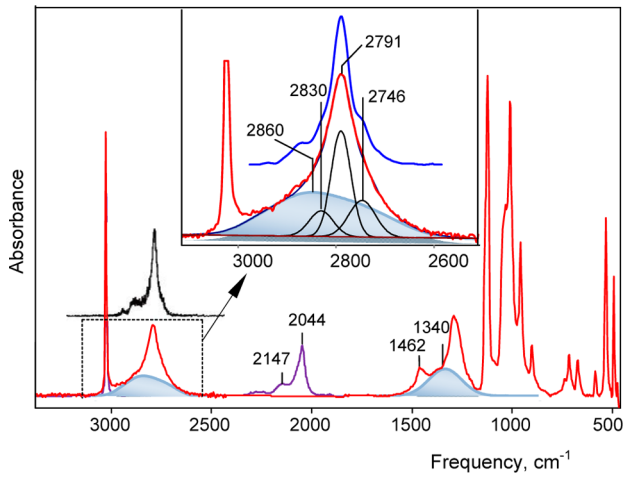

Figure 4. IR spectra of a single-crystal *t*-Bu$^+${Cl$_{11}^-$} salt (red), of its deuterated analog (violet), and of the gaseous *t*-Bu$^+$ cation[8] (black). The broad absorption at ca. 2860 and 1340 cm^{-1} is shown as shaded blue. The deconvoluted stretch CH frequencies are shown in the inset with a peak-enhanced absorption contour (blue) after application of Gaussian-shaped deconvolution, to better show maxima of the overlapping bands.

determine rotational structure, and the spectrum looks like a condensed-phase spectrum.

The similarity of IR spectra of *t*-Bu$^+$ in both phases suggests that their interpretation should be based on the unified principles consistent with the theoretical predictions for the gas-phase spectrum.[7,9,10] On the contrary, the gaseous- and condensed-phase spectra show an important difference: the narrow bands of stretch vibrations from "free" C−H bonds (unaligned with the p_z orbital), which are well visible in the gas-phase spectrum (at 3038−2913 cm^{-1}; Figure 3a), are replaced with broad absorption at ca. 2900 or 2860 cm^{-1} in the spectra of solid *t*-Bu$^+${F$_{11}^-$} (Figure 3b) and of the crystalline *t*-Bu$^+${Cl$_{11}^-$} salt (Figure 4, inset), respectively. The conjugated bend vibrations manifest themselves as a broad absorption, shown as a blue shaded peak at 1340 cm^{-1} in Figure 4. To date, these differences have either remained undetectable or been ignored.

Explanation of these changes requires a detailed X-ray structure of *t*-Bu$^+$ salts that can help to identify the relation between the cation structure and features of its IR spectra. In contrast to previously reported structural data on *t*-Bu$^+$ salts,[17,20,22] we obtained a high-resolution X-ray crystal structure of *t*-Bu$^+${Cl$_{11}^-$},[18] which allowed us to determine the H atom positions with certainty, sufficient to measure the C−C−H angles and direction of the C−H bond toward the Cl atoms of the ions.

Two CH$_3$ groups of *t*-Bu$^+$ have one C−H bond that is within 5° or 7° of optimal alignment with the vacant p_z orbital of the central C atom. Their C−C−H angles of 101.1° and 101.3° (Scheme 3) are even smaller than the calculated gas-phase value (103°).[8] This means that the spatial orientation of these two C−H bonds is optimal for hyperconjugation. At the same time, they formed monofurcated H-bonds with C−H···Cl angles ∼163° and at relatively short H···Cl distances: in the range 2.91−2.95 Å. The other four C−H bonds of these two CH$_3$ groups are directed between two Cl atoms of carborane ions and form weaker bifurcated H-bonds. The third CH$_3$ group has one C−H bond, which deviates by 10° from optimal alignment with the p_z orbital and forms the C−C−H angle of 106.6°, indicating that this bond undergoes weaker hyperconjugation. As a consequence, it forms the weaker bifurcated H-bond.[18] Two other C−H bonds of this group form bifurcated and mostly weak trifurcated H-bonds. Thus, the third CH$_3$ group, which we labeled as CH$_3$*, is not equivalent to the other two, undergoes weaker hyperconjugation, and forms weaker H-bonds.

The existence of two types of CH$_3$ groups confirmed the different lengths of C−C bonds in *t*-Bu$^+$. Two C−C bonds have equal lengths 1.451(1) and 1.452(1) Å, whereas the third bond, which is the one that forms the CH$_3$* group, is shorter: 1.443(1) Å. This difference is not caused by the distorting influence of the crystal packing because IR spectra of *t*-Bu$^+${Cl$_{11}^-$} in the crystal state and in liquid phases (discussed

Scheme 3. Bond Angle Evidence of Hyperconjugation of the C−H$_{4C}$ Bond in *t*-Bu$^+$

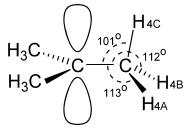

DOI: 10.1021/acs.jpca.5b04657
J. Phys. Chem. A XXXX, XXX, XXX−XXX

below) are the same. A similar result was observed in the X-ray structure of the *t*-Bu$^+$[$Al_2Br_7^-$] salt,[21] whose IR spectrum coincides with that of the melted salt and shows broad absorption due to the CH_3* group. Despite the greater error in the measurement of C−C distances, they are apparently different: two have almost equal length, 1.451(11) and 1.456(10) Å, and the third one is shortened: 1.431(11) Å.

The IR spectrum of the crystalline *t*-Bu$^+${Cl_{11}^-} salt (Figure 4) is consistent with its structure. First of all it does not contain the narrow bands of "free" C−H bonds. That is, in accordance with the X-ray data, all C−H bonds of *t*-Bu$^+$ are influenced by hyperconjugation and "solvation" with neighboring anions. The intense νCH_{max} band at 2791 cm^{-1} is a complex one. Its shape is not Gaussian because it contains the second band at 2746 cm^{-1} and possibly another one at 2830 cm^{-1}.The maxima of these bands are more clear-cut after application of Gaussian-shaped deconvolution (Figure 4, blue contour). The complex νCH_{max} band obviously corresponds to those CH stretches that are mostly involved in hyperconjugation and form the stronger H-bonds. We tentatively assigned the band with the lowest frequency at 2746 cm^{-1} (with weak-to-medium intensity) to vibrations of two C−H bonds that are best aligned for hyperconjugation and form the strongest monofurcated H-bonds. We labeled it as νCH_{align}. This assignment is arbitrary because the stretch vibration of the aligned C−H bond is not a characteristic one: all three CH stretch vibrations of the CH_3 group are significantly mixed. The majority of unaligned C−H bonds that form the bifurcated H-bonds should make a major contribution to the νCH_{max} absorption. This interpretation suggests that all three stretches of the CH_3 group are responsible for the complex νCH_{max} absorption.

The CH bend vibrations of *t*-Bu$^+$ conjugated with νCH_{max} manifest themselves as a complex band with a maximum at 1462 cm^{-1} (Figure 4).

The broad absorption pattern that we observed in the regions of C−H stretch and bend vibrations (shaded blue in Figure 4) is noteworthy because it derives from the absorption of "free" C−H bonds observed in the gaseous IR spectrum. To determine this absorption more accurately and to find other features of the IR spectrum of *t*-Bu$^+$, we analyzed the spectrum of the deuterated *t*-Bu$^+${Cl_{11}^-}-d_9 salt as well. It shows all the same C−D frequencies as those mentioned above for C−H, with the isotopic H/D ratio *ca.* 1.37 common for harmonic vibrations (Table 1). Calculation of the difference between the

Table 1. Frequencies of Protio- and Deuterio *t*-Bu$^+${Cl_{11}^-} Salts and the Isotopic H/D Ratio

	stretch vibrations of CX_3 groups		broadened absorption		νCC		
X	νCX_{max}	νCX_{alignx}	νCX	δCX			
H	**2791**[a]	2746	2860	1340	1333	**1291**	1262
D	**2044**	2011	2101	980	1164	**1125**	1092
H/D	**1.365**	1.365	1.362	1.368	1.145	**1.15**	1.155

[a]Boldface values denote strong bands.

spectra of protio- and deuterio-*t*-Bu$^+${Cl_{11}^-} salts under conditions of full subtraction of the {Cl_{11}^-} anion's absorption allowed us to identify the absorption of protio-*t*-Bu$^+$ as positive (above background) and of deuterio-*t*-Bu$^+$ as negative (below background, Figure 5).This difference distinctly shows broad "positive" and "negative" absorption patterns in the region of CH and CD bend vibrations, which were estimated with one

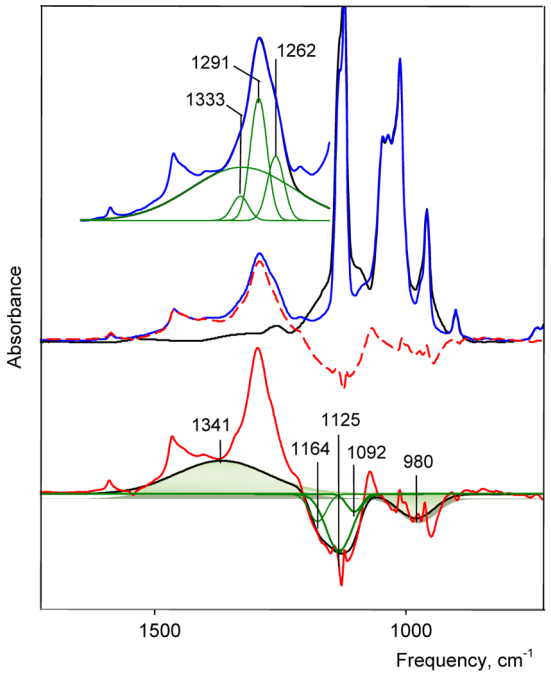

Figure 5. IR spectra of *t*-Bu{Cl_{11}} (blue) and *t*-Bu{Cl_{11}}-d_9 (black) with normalized intensity levels of {Cl_{11}^-}. Their difference (red dashed curve) is shown as separately scaled by 2Y (red bold curve) with "positive" absorption from protio-*t*-Bu$^+$ and "negative" absorption from deuterio-*t*-Bu$^+$. The broad C−H bend absorption is green; deconvolution of the bands of the νCC stretch is shown for the deuterio sample on the basis of the difference spectrum and for the protio sample in the inset at the top.

band at 1340 cm^{-1} of 230 cm^{-1} width in the protio sample, and at 980 cm^{-1} width 102 cm^{-1} in the deuterio sample. Their isotopic H/D ratio of 1.37 (Table 1) is in agreement with harmonic vibrations.

The difference spectrum allows for identification of frequencies corresponding predominantly to C−C stretches as well: We detected a three-component band at 1333, 1291, and 1262 cm^{-1} for protio-*t*-Bu$^+$ (Figure 5) with a low H/D ratio, ca. 1.15 (Table 1); this finding confirmed the assignment to the C−C stretches mixed with C−H bend vibrations.

The lack of broad absorption in the gas-phase spectrum is indicative of influence of the medium. Generally, broadening of IR bands is attributed to conformational inhomogeneity, when each molecule of a very large number may be H-bonded to a slightly different extent, just as νOH of liquid alcohols and phenols. In our case, the CH_3 groups of *t*-Bu$^+$ in the crystalline {Cl_{11}^-} salt form a limited number of nonequivalent H-bonds that can result in some additional broadening of the complex νCH_{max} band (half-width is ca. 100 cm^{-1}). Nevertheless, the width of the broad absorption of the CH stretches is much greater, ca. 300 cm^{-1}, and is reduced by half after deuteration. This result confirmed that the anomalous broadening is related to dynamic properties of the proton, and the mechanism differs from that of liquid alcohols and phenols.

We can explain the broadening effect by means of formation of bi- and trifurcated H-bonds. When C−H bonds of the CH_3 group are directed between two or three halogen atoms of carborane anions, the H atoms can fluctuate between two or three potential minima determined by each halogen atom involved in the H-bonding (Scheme 4). The potential barrier separating these minima is so low that the proton potential

DOI: 10.1021/acs.jpca.5b04657
J. Phys. Chem. A XXXX, XXX, XXX−XXX

Scheme 4. Proton Fluctuation between Two Minima, When It Forms a Bifurcated H-Bond

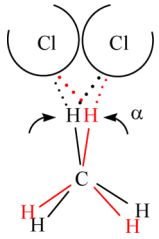

minimum is converted to one hole with a flat bottom. The hyperconjugation may not prevent the concerted libration of H atoms of CH_3 within the limits of a certain α-angle (Scheme 4), and then broadening of both stretch and bend C−H vibrations occurs. Earlier, we proposed a similar explanation for the strong broadening of N−H stretch vibration of the R_3NH^+ cation, when it forms a π-hydrogen bond with a double or triple CC bond of alkenes and alkynes:[34] The π-H bond, directed toward the center of the C═C or C≡C bond, is not fixed but fluctuates within a small range of some angle because the maximum of the π-electron density centered between the two carbon atoms is flat.

It is important to note that if the CH_3 group contains dynamic protons, *all* normal vibration of this group manifests itself as strongly broadened bands, which merge into one broad absorption pattern. In other words, the broad absorption patterns of vibrations from C−H stretches and bends correspond to at least one CH_3 group of *t*-Bu^+. Because this absorption from C−H stretches has a higher frequency than does νCH_{max}, it is reasonable to assume that it corresponds to vibrations of the third group (CH_3*), which is involved in the weakest hyperconjugative interaction and forms only bi- and trifurcated H-bonds.

IR spectra of all the *t*-Bu^+Carb^- salts analyzed have a characteristic feature: a broad absorption pattern (Figures 3, 4, and S3 [Supporting Information]). Its width and intensity depend on the size of halogen atoms of carborane ions (Table 2). For the salts with $\{F_{11}^-\}$ anions containing F atoms (the smallest radius), the width of the broad absorption pattern of C−H stretches is the smallest because the α-angle of H atom deviation is the smallest. The intensity of this broad absorption, relative to the total absorbance of C−H stretches, is 34% (Table 2), suggesting that only the CH_3* group is responsible for this absorption. The breadth of the absorption increases roughly 2-fold in the spectra of the salt with $\{Cl_{11}^-\}$ anions (ca. 250 cm^{-1}) and increases further up to 355 cm^{-1} in the salts with the brominated $\{Me_5Br_6^-\}$ anion. Simultaneously, the intensity of the broad absorption increases almost 2-fold, up to 60−65% and becomes more asymmetric (Figure S3 in the Supporting Informatino). Obviously, absorption of the second CH_3 group of *t*-Bu^+ is converted to a broad absorption pattern.

Table 2. Width and Relative Intensity (*I*) of the Broad Absorption of *t*-Bu^+ in the Region of C−H Stretch Vibrations (as a Percentage of the Total C−H Stretch Absorption) in the Salts with Various Counterions and Phase States[b]

	anion							
	$\{F_{11}^-\}$		$\{Cl_{11}^-\}$		$\{Me_5Cl_6^-\}$		$\{Me_5Br_6^-\}$	
phase	*I*	width	*I*	width	*I*	width	*I*	width
d_9 solid			34	115				
solid	34	122	55	250	60	300	66	355
liquid[a]			75	340				

[a] $[t\text{-}Bu^+\{Cl_{11}\}^-]_n$ associates forms in dichloroethane [b]The deuterated sample is denoted as d_9.

Dichloroethane Solutions. Solubility of the *t*-$Bu^+\{F_{11}^-\}$ salt in DCE-d_4 is low and the isolated spectrum of *t*-Bu^+, after subtraction of the spectrum of the solvent, showed an increased noise level. Nevertheless, this does not prevent identification of the main features of its C−H stretch vibrations (Figure S4 available in the Supporting Information). The spectrum shows a significant red shift of both νCH_{max} and νCH_{aling} bands relative to those of the solid salt (*ca.* 37−50 cm^{-1}; Table 3), indicating that *t*-Bu^+ is solvated by DCE, which is more basic than $\{F_{11}^-\}$ anions.[32] Therefore, the solvent-separated ion pairs, $(t\text{-}Bu^+)_{solv}\{F_{11}^-\}$, are formed. The spectra show a strong band at 637 cm^{-1} of the DCE-d_4 molecules that solvated the *t*-Bu^+ cation. This band disappeared when the solid *t*-$Bu^+\{F_{11}^-\}$ was recovered by evaporation of the solvent at room temperature. The weak intensity of the spectrum does not allow us to say with certainty whether it contains a broad absorption pattern. In any case, if it is present, its intensity is low.

Table 3. νCH_{max} and νCH_{aling} Frequencies of *t*-Bu^+ in Its Solid Salts and in Dichloroethane-d_4 Solutions (cm^{-1})

salt	phase	νCH_{max}	Δ^a	νCH_{aling}	Δ^a
t-$Bu^+\{F_{11}^-\}$	solid salt	2823		2766	
	DCE solution	2773	+50	2729	+37
t-$Bu^+\{Cl_{11}^-\}$	solid salt	2791		2745	
	DCE solution	2800	−9	2745	0

[a] Difference $\nu CH_{solid} - \nu CH_{solution}$.

Solubility of the *t*-$Bu^+\{Cl_{11}^-\}$ salt in DCE-d_4 is ∼10-fold higher than that of *t*-$Bu^+\{F_{11}\}^-$. The spectrum of the saturated solution of *t*-$Bu^+\{Cl_{11}^-\}$ is almost identical to that of the solid salt (Figure 6): the νCH_{max} and νCH_{aling} frequencies are indeed the same in both phases (Table 3) even though DCE is more basic than $\{Cl_{11}^-\}$ cations.[35] Meanwhile, the relative intensity of the band at 637 cm^{-1} of the DCE-d_4 molecules that solvated *t*-Bu^+ is several times weaker than that of $(t\text{-}Bu^+)_{solv}\{F_{11}^-\}$ solutions. All data indicate that in saturated solutions, the self-

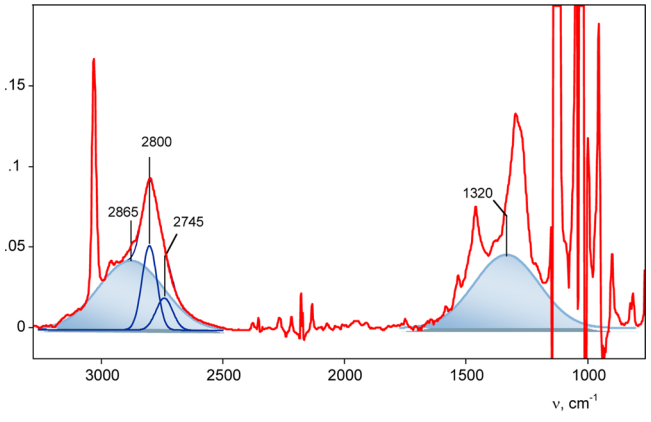

Figure 6. IR spectrum of the saturated solution of *t*-$Bu\{Cl_{11}\}$ in dichloroethane-d_4. The broad absorption is shown as shaded blue. The spectrum of the solvent is subtracted.

DOI: 10.1021/acs.jpca.5b04657
J. Phys. Chem. A XXXX, XXX, XXX−XXX

association takes place. The t-Bu$^+$ cations of $[t\text{-Bu}^+\{Cl_{11}\}^-]_n$ associates are mostly H-bonded with Cl$^-$ atoms of $\{Cl_{11}^-\}$ anions, and only a minority of their CH bonds are solvated by DCE molecules. For this reason, the spectrum shows a broad absorption pattern at ca. 2865 and ca. 1320 cm^{-1} (Figure 6), whose intensity is even higher than that of the solid t-Bu$^+\{Cl_{11}^-\}$ salt. Evaporation of a drop of this solution on the surface of a diamond crystal of the ATR accessory decreased the relative intensity of the broad absorption of C−H stretches from 75% for the liquid phase to 55% for the solid one (Table 2). Therefore, in the liquid phase, increased mobility of $\{Cl_{11}^-\}$ anions surrounding the t-Bu$^+$ cation enhanced the dynamic properties of H atoms of CH_3 groups, leading to dynamic broadening of the absorption of CH_3 groups of t-Bu$^+$. Thus, the broad absorption is one of the main features of the IR spectrum of t-Bu$^+$ in condensed phases.

The ^{1}H NMR spectrum of t-Bu$^+$ in DCE-d_4 solutions consists of one peak at 3.97 ppm for solvent-separated ion pairs $(t\text{-Bu}^+)_{solv}\{F_{11}^-\}$ or 4.03 ppm for associates $[t\text{-Bu}^+\{Cl_{11}^-\}]_n$. The t-Bu$^+$ cation shows a similar signal in the superacidic SbF_5 matrix, 4.35 ppm,[2,36,37] and in a SO_2 solution of t-Bu$^+(Sb_2F_{11})^-$: 4.24 ppm.[22] Thus, the quick proton exchange during NMR does not allow for detection of specific features of the t-Bu$^+$ structure in the liquid phase.

3.3. Contribution of H-Bonding and Hyperconjugation to Stabilization of the t-Bu$^+$ Cation. The cations of the t-Bu$^+$Carb$^-$ salts are H-bonded to anions that have decreasing C−H stretch frequencies.[18] It is possible to plot νCH_{max} against the anion basicity on the NH basicity scale (in cm^{-1}).[35] This scale is based on measurement of the νNH frequency of the contact ion pairs $Oct_3NH^+\cdots Anion^-$ in CCl_4 solutions relative to νNH of the $Oct_3NH^+\cdots CCl_4$ solvate in the solvent-separated ion pairs ($\Delta\nu$NH). The higher the anion basicity, the stronger is H-bonding and the greater is the low-frequency $\Delta\nu$NH shift. Within this scale, νNH of the $Oct_3NH^+\cdots CCl_4$ cation represents basicity of CCl_4, which was assumed to be zero. It is important, however, to plot the dependencies starting from naked t-Bu$^+$ in vacuum, that is, from real zero basicity of the medium. This approach necessitates analysis of the basicity of CCl_4 relative to vacuum. The νNH frequencies of $Oct_3NH^+\cdots CCl_4$ and Oct_3NH^+ in vacuum were calculated on the basis of the B3LYP/6-31G** level (3424 and 3376 cm^{-1}, respectively) and their difference, 48 cm^{-1}, represents the basicity of CCl_4. We expected that calculations at different levels would result in some variation of νNH values of both species but would not noticeably change the difference between the two values.

The plotted dependence of νCH_{max} on anion basicity is shown in Figure 7 (black bold curve). When the basicity increases from −48 (vacuum) to +50 cm^{-1}, the slope is close to zero, then progressively increases reaching a constant value at basicity above 100 cm^{-1}. A linear function of the least-squares fit of the five νCH_{max} data points (2−6 in Figure 6, red) was extrapolated to zero basicity (for vacuum) at the frequency of 2954 cm^{-1}, which coincides with asymmetric vibrations of CH_3 groups of gaseous $C(CH_3)_4$. These results mean that asymmetric vibration of the "free" CH_3 group of t-Bu$^+$, in the absence of hyperconjugation and H-bonding, should be almost identical to that of $(CH_3)_4C$, as expected. Participation of the CH_3 group of t-Bu$^+$ in hyperconjugation allows it to form H-bonds with the basic immediate environment of the condensed phase. With increasing basicity in the 100−150 cm^{-1} range, strengthening of the H-bonds enhanced hyperconjugation and vice versa; i.e., they proportionally reinforce each other. This

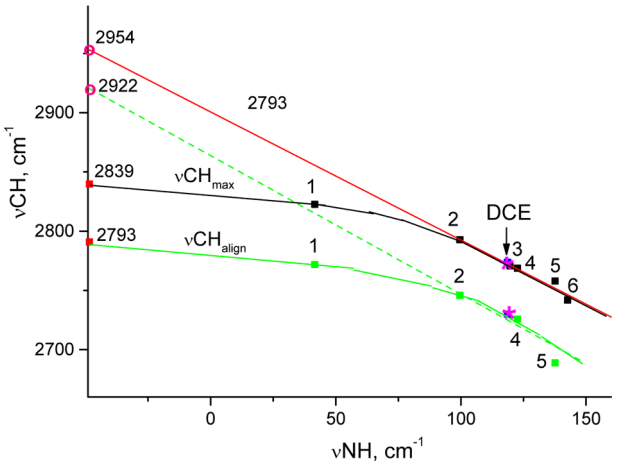

Figure 7. Dependences of νCH_{max} (black bold curve) and νCH_{align} frequencies (green bold curve) of t-Bu$^+$ on the basicity of anions: $\{F_{11}^-\}$ (1), $\{Cl_{11}^-\}$ (2), $\{Me_5Cl_6^-\}$ (3), $\{Br_{11}^-\}$ (4), $\{H_5Br_6^-\}$ (5), and $\{Me_5Br_6^-\}$ (6). Red dots indicate experimental data on gas-phase t-Bu$^+$,[8] two pink circles correspond to ν_sCH_3 and $\nu_{as}CH_3$ of gaseous $(CH_3)_4C$, and two magenta asterisks to a solvated t-Bu$^+$ cation in dichloroethane. The linear function of the least-squares fit of the five νCH_{max} data points is shown as a red line.

finding means that νCH_{max} represents the same type of normal vibrations of CH_3 groups as does $\nu_{as}CH_3$ of $(CH_3)_4C$.

A similar dependence on the anion basicity was uncovered in the plot of the νCH_{align} frequency. Because the νCH_{align} band overlaps with the more intense νCH_{max} component, the error of its measurement increased and fewer points had to be used in the plot: those whose maximum was determined with appropriate accuracy (±3 cm^{-1}). Another difficulty is that the νCH_{align} band has not been identified in the published spectrum of the gaseous t-Bu$^+$ cation.[8] Nevertheless, the deconvoluted νCH_{max} band of the gaseous t-Bu$^+$ cation clearly indicates that it comprises two additional bands (Figure 3a). One, with the lowest frequency, is at 2793 cm^{-1}. Addition of this data point to the νCH_{align} values plotted against anion basicity resulted in a dependence almost identical to that of νCH_{max} (Figure 7, green).

The fewer points in the νCH_{align} dependence and their greater scatter did not allow us to construct a linear function of a least-squares fit with extrapolation to zero basicity. Nonetheless, to demonstrate that the two dependencies are identical, we should assume that the linear part of the νCH_{align} dependence starts at 2922 cm^{-1} for ν_sCH_3 of $(CH_3)_4C$. That is, the νCH_{align} frequency results from the symmetric vibration of the unperturbed "free" CH_3 group.

The high similarity of the two dependences in Figure 7 indicates that νCH_{max} and νCH_{align} represent asymmetric and symmetric C−H stretch vibrations, respectively, of those two CH_3 groups of t-Bu$^+$ that undergo strong hyperconjugation, regardless of whether t-Bu$^+$ is naked in vacuum or solvated in a condensed phase. This is an important finding of the present study.

Two graphs shown in Figure 7 can be supplemented with the data points corresponding to the solvated $(t\text{-Bu}^+)_{solv}$ cation in DCE. The basicity of DCE molecules on the NH basicity scale has been reported (119 cm^{-1}),[32] and νCH_{max} and νCH_{align} of $(t\text{-Bu}^+)_{solv}$ are shown in the graphs of Figure 7 as magenta asterisks. They fitted well to both dependences, confirming that

DOI: 10.1021/acs.jpca.5b04657
J. Phys. Chem. A XXXX, XXX, XXX−XXX

Table 4. Comparison of the Calculated Frequencies with Empirical Data

νCH_{max} band	**Calc**: νCH_{max} band consists of three C−H frequencies separated by **12** cm^{-1} (Table S1, Supporting Information), which correspond to stretch vibrations of **three** C−H bonds from **three** CH_3 groups aligned with the p_z orbital. **Experiment**: νCH_{max} band contains three C−H stretches of **one** type of CH_3 group, separated by **ca. 40−60** cm^{-1} (Figure 3).	complete mismatch
CH stretches of $(CH_3)_3C^+$ versus $(CH_3)_4C$	**Calc**: The blue shift of νCH (the rehybridization effect exceed the effect of hyperconjugation) is **13** cm^{-1} **Experiment**: **60** cm^{-1} **Calc**: The red shift of νCH_{max} from hyperconjugation is **47** cm^{-1} **Experiment**: **140** cm^{-1}	unacceptable difference
influence of the medium and solvation by Ar	**Calc**: The medium decreases all C−H stretches by **11−15** cm^{-1} (Table S1, SupportingInformation). Solvation by Ar decreases first of all the νCH_{max} by **35−39** cm^{-1} and the other CH stretches to a slightly smaller extent (Table S2, SupportingInformation). **Experiment**: Solvation with $\{F_{11}^-\}$ (basicity is comparable with that of Ar) decreases νCH_{max} by **10** cm^{-1} and decreases the other CH stretches by **120** cm^{-1}.	drastic mismatch

Table 5. CH Stretch Frequencies of Unhyperconjugated CH_3 Groups of Some Cations and Neutral Molecules in Comparison with Those of the CH_3* Group of the Gaseous *t*-Bu^+

compound	phase	$\nu_{as}CH_3$	$\nu_{as}CH_3$*/$\nu_{as}CH_3$	ν_sCH_3	ν_sCH_3*/ν_sCH_3	ref
$(CH_3)_3C^+$	gas	3036[a]		2965[a]		8
$(CH_3)_4C$	gas	2954, 2963	1.026 (av)	2922	1.015	40
$(CH_3)_3CCl$	gas	2981	1.018	2937	1.009	41
CH_3Cl	gas	3042	0.998	2966	1.000	42
$[CH_3Cl^+CH_3]\{Cl_{11}\}^-$	solid	3068	0.989	2957	1.002	43
$CH_3^+\{Cl_{11}\}^-$	solid	3084, 3071	0.987 (av)	2962	1.001	43
$[(CH_3)_2CH_2CH_3^\star]^+\{Cl_{11}\}^-$	solid	3040[b]	0.999	2967[b]	0.999	39
$(CH_3)_3B$	gas	2975	1.0205	2875	1.031	44

[a] $\nu_{as}CH_3$* and ν_sCH_3* frequencies of the CH_3* group of the $(CH_3)_3C^+$ cation; [b] ν_{as} and ν_s of the marked $CH_3^\star$ group of the $[(CH_3)_2CH_2CH_3^\star]^+$ cation.

in DCE, solvent-separated ion pairs $(t\text{-}Bu^+)_{solv}\{F_{11}^-\}$ are formed.

Dependencies shown in Figure 7 prove that the IR spectra (and structures) of *t*-Bu^+ in all phases are strongly related.

3.4. Structure and IR Spectra of the *t*-Bu^+ Cation: The Experiment versus Calculations. The IR spectrum of gaseous *t*-Bu^+ was measured for tagged species, $C_4H_9^+Ar$.[9] The binding of Ar to $C_4H_9^+$ affects the spectrum of the cation. In ref #9, the empirical spectrum was compared with a calculated one for untargeted $C_4H_9^+$ with a C_s conformation. Those researchers found that this spectrum is in good agreement with empirical data. The same would be true in the present study if we assumed that three of the six empirical bands—2913, 2880, and 2793 cm^{-1} (Figure 3a)—are absent or do not correspond to C−H stretch vibrations. The calculated spectra of the two $C_4H_9^+Ar$ species with Ar bound to the CH_3 group or to the central C atom are close to that of neat $C_4H_9^+$ (C_s) and represent a somewhat worse fit to the empirical spectrum (Figure S2 and Table S2 in the Supporting Information). Again, we must assume the absence of the three above-mentioned bands.

It is possible to interpret the spectrum of gaseous $C_4H_9^+Ar$ on the condition that Ar is attached to the CH_3* group, which primarily interacts with the medium when the cation is transferred to the condensed phase. The C−H stretch of CH···Ar has the lowest frequency, 2913 cm^{-1}, and two other C−H bonds are responsible for 3038 and 2965 cm^{-1} bands (Figure 3a). Consequently, all the stretch vibrations—three from CH_3* and three from the other two equivalent CH_3 groups—were observed in the spectrum with reasonable frequencies and were successfully interpreted in the present work.

Some other notable discrepancies between the calculated and empirical spectra are provided in Table 4. They confirm that the calculated structure of *t*-Bu^+ does not correspond to the empirically determined one because of the different charge redistributions among the three CH_3 groups. One group, CH_3*, in comparison with the other two, is less involved in hyperconjugation, and this situation is compensated by stronger polarization. This state of affairs explains the distinctive features of CH_3*: the higher frequencies of C−H stretches and enhanced dynamic properties of the protons, leading to the strong broadening of its absorption pattern in condensed phases. Depending on the immediate environment, the complex νCH_{max} band of the second and third CH_3 groups can also be transformed into broad absorption.

The influence of polarization on the electron density distribution in *t*-Bu^+ has been examined by Schleyer at al.[38] by means of calculations at the MP2/6-31G* level. They found that a positive charge decreases the e^--density of the hydrogens and carbon p-orbitals, whereas the e^--density was gained by the other carbon orbitals onto C−C and C−H bonds. As a result, the e^--density of these bonds increased, also increasing their stretch vibrations. For example, the increasing positive charge on the methyl group in the following series: $(CH_3)_4C$, $(CH_3)_3CCl$, CH_3Cl, $[CH_3Cl^+CH_3]\{Cl_{11}\}^-$, and $CH_3^+\{Cl_{11}\}^-$, is accompanied by increasing $\nu_{as}CH_3$ (Table 5), which can serve as a measure of CH_3 polarizability. Thus, $\nu_{as}CH_3$* and ν_sCH_3* of gaseous *t*-Bu^+ actually are identical to those of gaseous methyl chloride and the $CH_3^\star$ group of the 2-methylbutyl cation,[39] which is not perturbed by hyperconjugation (Table 5). A good correlation was observed here for C−H stretches of CH_3* and methyl groups of isoelectronic planar trimethylboron, $(CH_3)_3B$, confirming the identical e^--redistribution among their methyl groups (Table 5). In general,

DOI: 10.1021/acs.jpca.5b04657
J. Phys. Chem. A XXXX, XXX, XXX−XXX

a similar good correlation is observed among all compounds listed in Table 5.

According to the above results, a hyperconjugative interaction of the two CH_3 groups of *t*-Bu^+ with the p_z orbital of the central C atom leads to donation of the e^- density from their hybridized molecular orbitals (i.e., from all three σ-C−H bonds) via the aligned C−H bond to the up and down p_z lobes of the p_z orbital (Scheme 5). The weakening of the C−H bonds

Scheme 5. E-Density Donation from σ-MOs of CH_3 Groups to the p_z Orbital of the sp^2 C Atom and C−C Bonds of *t*-Bu^+

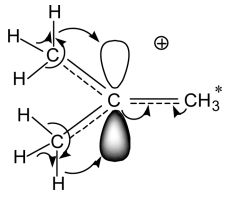

of CH_3 groups results in red shifting of C−H stretches by 140 cm^{-1} on average, in comparison with tetramethylmethane (Figure 8). The third CH_3* group is mostly polarized (Scheme 5), with blue shifting of its C−H stretches by ca. 60 cm^{-1} (Figure 8).

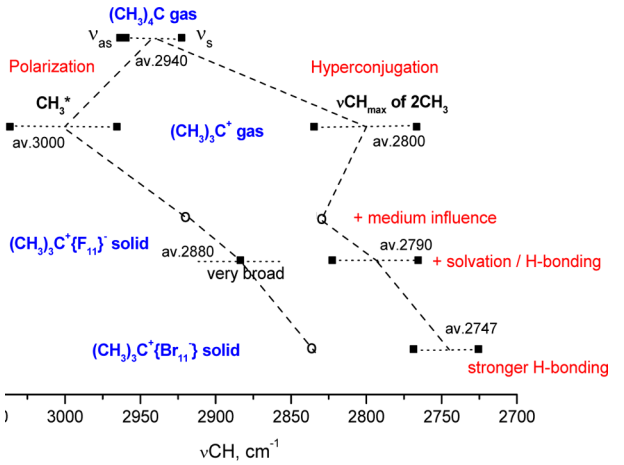

Figure 8. Correlation diagram for stretch vibrations of CH_3 groups of $(CH_3)_4C_{(gas)}$ and the $(CH_3)_3C^+_{(gas)}$ cation, which is then transferred to solid *t*-Bu^+ salts. The circles denote the proposed frequencies.

The transfer of $(CH_3)_3C^+$ from a gaseous to condensed phase leads to participation of the polarized CH_3* group in hyperconjugation; this change significantly decreases the stretch vibrations. Simultaneously, by the law of energy conservation, the hyperconjugation strengths of the other two CH_3 groups should diminish and their νCH_{max} should increase, as shown in the diagram of Figure 8 (the circles). At the same time, the solvation effect and H-bonding tend to decrease all C−H stretches; this effect compensates or slightly overlaps with the νCH_{max} increase caused by the previous effect. As a result, the νCH_{max} is changed insignificantly (even decreased by ca. 7 cm^{-1}) (Figure 8, example $(CH_3)_3C^+\{F_{11}^-\}$). With the increasing basicity of the immediate environment and with strengthening H-bonds, the νCH frequencies continue to decrease, enhancing hyperconjugation (Figure 8, the example $(CH_3)_3C^+\{Br_{11}^-\}$).

The disagreement between the calculated IR spectrum of optimized *t*-Bu^+ structures with the empirical one is possible if calculations overestimate the spatial size of the p_z and σ orbitals of the *t*-Bu^+ cation; this situation may lead to overestimation of the overlap of the orbitals. In this case, the hyperconjugation strength should be less dependent on variation of the dihedral angle between an aligned C−H bond and an empty p_z orbital than could be expected from the experimental data. Another possible reason is that the software used cannot accurately account for the effect of polarization.

4. CONCLUSIONS

In the present work, we propose a unified concept of *t*-Bu^+ stabilization in gaseous, liquid, and solid phases. This concept is based on the combined data from IR spectra and X-ray crystallographic structure of the *t*-$Bu^+\{Cl_{11}^-\}$ salt, the similarity of IR spectral features of *t*-Bu^+ in the gaseous and condensed phases, and their dependence on formation of an H-bond with neighboring bases. This concept has the following implications: (1) *t*-Bu^+ contains two types of nonequivalent CH_3 groups: one, CH_3*, is presumably polarized, and the other two are involved in strong hyperconjugation; (2) both hyperconjugation and polarization play a key role in *t*-Bu^+ stabilization; efficiency of the charge distribution among both types of CH_3 groups is comparable.

In the gas phase, the CH_3* group is mostly polarized. In condensed phases, under conditions of negligible H-bonding, the influence of a dielectric medium and electrostatic solvation on *t*-Bu^+ promotes participation of the polarized CH_3* group in hyperconjugation, which decreases the frequencies of its C−H stretches by ca. 120 cm^{-1}. At the same time, weakening of hyperconjugation of the other two CH_3 groups is compensated by the effect of solvation, which ultimately leads to an insignificant change in their C−H stretches. This phenomenon results in efficient scattering of the positive charge to the medium and in further stabilization of the cation. The formation of H-bonds between *t*-Bu^+ and counterions enhances hyperconjugation and cation stabilization, while maintaining the nonequivalence of the methyl groups.

In the future, we are planning to demonstrate applicability of the proposed concept to interpretation of the spectral features of saturated C1−C6 carbocations.

■ ASSOCIATED CONTENT

Supporting Information

Calculated optimized structures and energies of neat *t*-Bu^+ and *t*-Bu^+ solvated with Ar in vacuum, calculation with the IEFPCM solvent model, calculated IR spectra, additional experimental IR spectra of *t*-Bu^+ in condensed phases. The Supporting Information is available free of charge on the ACS Publications website at DOI: 10.1021/acs.jpca.5b04657.

■ AUTHOR INFORMATION

Corresponding Author

*E. S. Stoyanov. Phone: +7 383 330 5573. E-mail: evgenii@nioch.nsc.ru.

Notes

The authors declare no competing financial interest.

■ ACKNOWLEDGMENTS

We are grateful to the Ministry of Education and Science of the Russian Federation for the support within the Project of the

DOI: 10.1021/acs.jpca.5b04657
J. Phys. Chem. A XXXX, XXX, XXX−XXX

joint Laboratories of the Siberian Branch of the Russian Academy of Sciences and National Research Universities. The authors thank Prof. Igor V. Alabugin for NBO analysis of the *t*-Bu^+ cation, Prof. Paul von Rague Schleyer for useful advice, and Irina S. Stoyanova for providing the carborane acids and technical support.

REFERENCES

(1) Olah, G. A.; Molnar, A. *Hydrocarbon Chemistry*; John Wiley & Sons: New York, 2003.
(2) Olah, G. A.; Baker, E. B.; Evans, J. C.; Tolgyesi, W. S.; McIntyre, J. S.; Bastien, I. J. Stable Carbonium Ions. V. Alkylcarbonium Hexafluoroantimonates. *J. Am. Chem. Soc.* **1964**, *86*, 1360−1373.
(3) Olah, G. A.; Lukas, J. Stable Carbonium Ions. XLVII. Alkylcarbonium Ion Formation From Alkanes via Hydride (Alkide) Ion Abstraction in Fluorosulfonic Acid-Antimony Pentafluoride-Sulfuryl Chlorofluoride Solution. *J. Am. Chem. Soc.* **1967**, *89*, 4739−4744.
(4) Prakash, G. K. S., Schleyer, P. v. R., Eds. *Stable Carbocation Chemistry*; John Wiley & Sons: New York, 1997.
(5) Olah, G. A., Prakash, G. K. S., Eds. *Carbocation Chemistry*; John Willey & Sons: Hoboken, NJ, 2004.
(6) Weigend, F.; Ahrichs, R. Balanced Basis Sets of Split Valence, Triple Zeta Valence and Quadruple Zeta Valence Quality for H to Rn: Design and Assessment of Accuracy. *Phys. Chem. Chem. Phys.* **2005**, *7*, 3297−3305.
(7) Feng, H.; Sun, W.; Xie, Y.; Schaefer, H. F. Structures and Energetics of the tert-Butyl Cation: The Final Answer or a Never-Ending Story? *Chem. - Eur. J.* **2011**, *17*, 10552−10555.
(8) Douberly, G. E.; Ricks, A. M.; Ticknor, B. W.; Schleyer, P v.R.; Duncan, M. A. Infrared Spectroscopy of the tert-Butyl Cation in the Gas Phase. *J. Am. Chem. Soc.* **2007**, *129*, 13782−13783.
(9) Sieber, S.; Buzek, P.; Schleyer, P. v. R.; Koch, W. J.; Carneiro, W. de M. The tert-Butyl Cation ($C_4H_9^+$) Potential Energy Surface. *J. Am. Chem. Soc.* **1993**, *115*, 259−270.
(10) Rasul, G.; Chen, J. L.; Prakash, G. K. S.; Olah, G. A. Ab Initio/DFT/GIAO−CCSD(T) Calculational Study of the *t*-Butyl Cation: Comparison of Experimental Data with Structures, Energetics, IR Vibrational Frequencies, and ^{13}C NMR Chemical Shifts Indicating Preferred C_sConformation. *J. Phys. Chem. A* **2009**, *113*, 6795−6799 and references therein.
(11) Wu, J. I-C.; Schleyer, P. v. R. Hyperconjugation in Hydrocarbons: Not Just a "Mild Sort of Conjugation". *Pure Appl. Chem.* **2013**, *85*, 921−940.
(12) Baer, T., Ng, C.-Y., Powis, I., Eds. *The Structure, Energetics and Dynamics of Organic Ions*; John Wiley & Sons: Chichester, U.K., 1996.
(13) Holmes, J. L.; Aubrey, C.; Mayer, P. M. *Assigning Structures to Ions in Mass Spectrometry*; CRC Press: Boca Raton, FL, 2007.
(14) Duncan, M. A. Infrared Laser Spectroscopy of Mass-Selected Carbocations. *J. Phys. Chem. A* **2012**, *116*, 11477−11491.
(15) Alabugin, I. V.; Manoharan, M. Rehybridization as a General Mechanism for Maximizing Chemical and Supramolecular Bonding and a Driving Force for Chemical Reactions. *J. Comput. Chem.* **2007**, *28*, 373−390.
(16) Alabugin, I. V.; Brescha, S.; Gomesa, G. P. Orbital Hybridization: A Key Electronic Factor in Control of Structure and Reactivity. *J. Phys. Org. Chem.* **2015**, *28*, 147−162.
(17) Olah, G. A.; Prakash, G. K. S.; Molnar, A.; Sommer, J. *Superacid Chemistry*, 2nd ed., Wiley: Hoboken, NJ, 2009.
(18) Stoyanov, E. S.; Stoyanova, I. V.; Tham, F. S.; Reed, C. A. Evidence for C-H Hydrogen Bonding in Salts of tert-Butyl Cation. *Angew. Chem., Int. Ed.* **2012**, *51*, 9149−9151.
(19) Laube, T. X-ray Crystal Structures of Carbocations Stabilized by Bridging or Hyperconjugation. *Acc. Chem. Res.* **1995**, *28*, 399−405 and references cited therein.
(20) Kato, T.; Reed, C. A. Putting *tert*-Butyl Cation in a Bottle. *Angew. Chem., Int. Ed.* **2004**, *43*, 2908−2911.
(21) Scholz, F.; Himmel, D.; Scherer, H.; Krossing, I. Superacidic or Not...? Synthesis, Characterisation, and Acidity of the Room-Temperature Ionic Liquid $[C(CH_3)_3]^+$ $[Al_2Br_7]^-$. *Chem. - Eur. J.* **2013**, *19*, 109−116.
(22) Hollenstein, S.; Laube, T. Crystal Structure of the tert-Butyl Cation. *J. Am. Chem. Soc.* **1993**, *115*, 7240−7245.
(23) Reed, C. Carborane Acids. New "Strong yet Gentle" Acids for Organic and Inorganic Chemistry. *Chem. Commun.* **2005**, 1669−1677.
(24) Juhasz, M.; Hoffmann, S.; Stoyanov, E. S.; Kim, K.; Reed, C. A. The Strongest Isolable Acid. *Angew. Chem., Int. Ed.* **2004**, *43*, 5352−5355.
(25) Nava, M.; Stoyanova, I. V.; Cummings, S.; Stoyanov, E. S.; Reed, C. A. The Strongest Brønsted Acid: Protonation of Alkanes by $H(CHB_{11}F_{11})$ at Room Temperature. *Angew. Chem., Int. Ed.* **2014**, *53*, 1131−1134.
(26) Frisch, M. J.; Trucks, G. W.; Schlegel, H. B.; Scuseria, G. E.; Robb, M. A.; Cheeseman, J. R.; Scalmani, G.; Barone, V.; Mennucci, B.; Petersson, G. A.; et al. *Gaussian 09*, revision D.01; Gaussian Inc.: Wallingford, CT, 2009.
(27) Andrienko, G. A. *ChemCraft*, http://www.chemcraftprog.com (accessed in 08/07/2015).
(28) Legault, C. Y. *CYLview*, Université de Sherbrooke, 2009 (http://www.cylview.org) (accessed in 08/07/2015).
(29) Reed, E.; Weinhold, F. Natural Localized Molecular Orbitals. *J. Chem. Phys.* **1985**, *83*, 1736−1740.
(30) Alabugin, V.; Manoharan, M.; Peabody, S.; Weinhold, F. Electronic Basis of Improper Hydrogen Bonding: A Subtle Balance of Hyperconjugation and Rehybridization. *J. Am. Chem. Soc.* **2003**, *125*, 5973−5987.
(31) Cancès, E.; Mennucci, B.; Tomasi, J. A New Integral Equation Formalism for the Polarizable Continuum Model: Theoretical Background and Applications to Isotropic and Anisotropic Dielectrics. *J. Chem. Phys.* **1997**, *107*, 3032−3041.
(32) Tomasi, J.; Mennucci, B.; Cancès, E. The IEF Version of the PCM Solvation Method: an Overview of a New Method Addressed to Study Molecular Solutes at the QM ab Initio Level. *J. Mol. Struct.: THEOCHEM* **1999**, *464*, 211−226.
(33) Tomasi, J.; Mennucci, B.; Cammi, R. Quantum Mechanical Continuum Solvation Models. *Chem. Rev.* **2005**, *105*, 2999−3094.
(34) Stoyanov, E. S.; Stoyanova, I. V.; Reed, C. A. The Basicity of Unsaturated Hydrocarbons as Probed by H-Bond Acceptor Ability. Bifurcated N−$H^+\cdots\pi$ Hydrogen Bonding. *Chem. - Eur. J.* **2008**, *14*, 7880−7890.
(35) Stoyanov, E. S.; Kim, K-Ch.; Reed, C. A. An Infrared νNH Scale for Weakly Basic Anions. Implications for Single-Molecule Acidity and Superacidity. *J. Am. Chem. Soc.* **2006**, *128*, 8500−8508.
(36) Olah, G. A.; Tolgyesi, W. S.; Kuhn, S. J.; Moffatt, M. E.; Bastien, I. J.; Baker, E. B. Stable Carbonium Ions. IV. Secondary and Tertiary Alkyl and Aralkyl Oxocarbonium Hexafluoroantimonates. Formation and Identification of the Trimethylcarbonium Ion by Decarbonylation of the *tert*-Butyl Oxocarbonium Ion. *J. Am. Chem. Soc.* **1963**, *85*, 1328−1334.
(37) Olah, G. A.; Donovan, D. J. Stable carbocations. 208. Carbon-13 Nuclear Magnetic Resonance Spectroscopic Study of Alkyl Cations. The Constancy of Carbon-13 Nuclear Magnetic Resonance Methyl Substituent Effects and Their Application in the Study of Equilibrating Carbocations and the Mechanism of Some Rearrangements. *J. Am. Chem. Soc.* **1977**, *99*, 5026−5039.
(38) Wiberg, K. B.; Schleyer, P. v. R.; Streitwieser, A. The Role of Hydrogens in Stabilizing Organic Ions. *Can. J. Chem.* **1996**, *74*, 892−900.
(39) Reed, C. A.; Stoyanov, E. S.; Tham, F. S. Hydrogen Bonding Versus Hyperconjugation in Condensed-Phase Carbocations. *Org. Biomol. Chem.* **2013**, *11*, 3797−3802.
(40) Evans, J. C.; Bernstein, H. J. The Vibrational Spectra of Isobutane and Isobutane-d_1. *Can. J. Chem.* **1956**, *34*, 1037−1045.
(41) Evans, J. C.; Lo, G.Y.-S. The Vibrational Spectra and Assignments of t-Butyl Chloride and t-Butyl-d_9 Chloride, and the

DOI: 10.1021/acs.jpca.5b04657
J. Phys. Chem. A XXXX, XXX, XXX−XXX

Calculated Ionization-Equilibrium, Deuterium-Isotope Effect. *J. Am. Chem. Soc.* **1966**, *88*, 2118−2122.
(42) Nakamoto, K. *Infrared and Raman Spectra of Inorganic and Coordination Compounds*, 5th ed.; John Wiley & Sons, Inc.: New York, 1997.
(43) Stoyanov, E. S.; Stoyanova, I. V.; Tham, F. S.; Reed, C. A. Dialkyl Chloronium Ions. *J. Am. Chem. Soc.* **2010**, *132*, 4062−4063.
(44) Lehmann, W. J.; Wilson, C. O.; Shapiro, I. Infrared Spectra of Trimethylborane-d_9 and Triethylborane-d_{15}. *J. Chem. Phys.* **1959**, *31*, 1071−1975.

DOI: 10.1021/acs.jpca.5b04657
J. Phys. Chem. A XXXX, XXX, XXX−XXX